

Structure of phosphorus clusters using simulated annealing— P_2 to P_8

R. O. Jones and D. Hohl

Institut für Festkörperforschung, Forschungszentrum Jülich, D-5170 Jülich, Federal Republic of Germany

(Received 11 December 1989; accepted 19 February 1990)

The geometries of low-lying isomers of phosphorus clusters P_2 to P_8 have been calculated using a density functional (DF) method, combined with molecular dynamics (MD) and simulated annealing techniques. The structures and vibration frequencies are in excellent agreement with experiment in those cases (P_2 , P_4) where spectroscopic data are available. A roof-shaped tetramer is a prominent structural unit in low-lying states of P_5 , P_6 , P_7 , and P_8 . Contrary to widespread belief, the most stable isomer of P_8 is not cubic, but the “wedge” or “cradle” structure found as a structural unit in violet (monoclinic, Hittorf) phosphorus. The energetic ordering and geometrical shapes of the P_8 isomers show striking analogies to the corresponding valence-isoelectronic hydrocarbons (CH)₈ cubane, cuneane, and 2,2':4,4'-bis-(bicyclobutyl). The bonding and structural trends in phosphorus clusters are discussed in detail.

I. INTRODUCTION

Phosphorus shows a structural variety in elemental form exceeded only by sulphur, its neighbor in the Periodic Table.¹⁻³ It is not surprising then that there have been many studies of the allotropes as well as amorphous phosphorus. The structures of four of the crystalline forms [black (orthorhombic), violet (monoclinic, Hittorf), rhombohedral, metallic (cubic)] are well established and there are numerous others known collectively as “red phosphorus.” There are two stable forms of white phosphorus (hexagonal below -77°C , cubic otherwise), both comprising tetrahedral P_4 molecules. White phosphorus is thermodynamically the least stable allotrope and transforms to the red form under the action of heat, light, or X radiation. P_4 tetramers are also important components of liquid phosphorus at moderate temperatures.

While both phosphorus and sulphur show a great variety of solid state structures, their gas phases show significant differences. Mass spectroscopy of sulphur vapor shows the presence of clusters of all sizes up to S_{56} ,⁴ and the formation of allotropes with ringlike molecular units (S_{6-13} , S_{18} , S_{20}) means that numerous structures can be determined by x-ray structural analysis (S_n , for $n = 6-8, 10-13, 18, 20$).⁵ For many years, however, phosphorus vapor showed a very small range of cluster sizes. The most prominent component is P_4 ,⁶⁻¹⁰ whose tetrahedral structure was inferred from Raman spectroscopy of liquid phosphorus by Bhagavantam,¹¹ calculated by Hultgren¹² and confirmed by electron diffraction measurements¹³ many years ago. The only other molecules to be identified for temperatures between 100 and 300°C were P_2 , P_3 , and P_8 ,^{6,8} and the last of these was not evident at higher temperatures.^{9,10} P_4 dissociates into dimers above 800°C ,^{3,10} and P_2 and P_4 are present in approximately equal numbers at 1770°C .³ At low temperatures, however, there are more similarities with sulphur vapor. Martin¹⁴ has shown recently that quenching of the vapor of red phosphorus in helium gas leads to P_n clusters of all sizes up to $n = 24$.

The stability of P_4 ¹⁵ and the apparent instability of larger clusters, particularly P_8 , have provided a continuing puzzle for several decades. With a valence configuration of

$3s^2 3p_x 3p_y 3p_z$, phosphorus is often expected to favor bond angles near 90° , as in phosphene (PH_3). If this is true, the strain energy present in tetrahedral bonds (bond angle $\alpha = 60^\circ$) should make them unfavorable. This problem has been addressed in calculations of P_2 and P_4 ^{10,16-18} and in calculations comparing bond strengths in P_2 , P_4 , and P_8 ¹⁹⁻²⁵. These calculations have been restricted, however, to the tetrahedral (T_d) form of P_4 and the cubic (O_h) form of P_8 . The most detailed calculations indicate that cubic P_8 is substantially less stable than two tetramers, but there has been no systematic attempt to determine P_8 structures with lower energies.

Ring and chain structures containing phosphorus have been studied extensively in recent years, with particular focus on the analogies with carbon, hydrocarbon,²⁶ and nitrogen chemistry. In the present context, we note examples such as the preparation of the planar P_5^- ion,²⁷ the P_6 analog of benzene,²⁸ and the P_7^- ion.^{3,29} The last of these is a fluctuating molecule²⁶ and provides an example of valence bond tautomerism, where equilibrium exists between structures with similar geometries, but different bonding. In the solid state, the violet (monoclinic) allotrope of phosphorus comprises alternating P_8 and P_9 “cages,” linked by pairs of phosphorus atoms to form tubes of pentagonal cross section.^{1,30,31} There are indications that amorphous red phosphorus also contains cagelike P_8 clusters,³² and Elliott *et al.*³² pointed out the possibility that they could form by polymerization of two P_4 molecules, with minimal atomic movement.

In spite of continuing interest in phosphorus clusters, there are many unanswered questions, even concerning such basic problems as the structure or even the stability of small clusters. In addition to the work mentioned above, first principle calculations have been performed for P_3 ^{33,34} (C_{2v} , a Jahn-Teller distorted D_{3h} structure) and for several forms of P_6 .^{35,36} Modified neglect of diatomic overlap (MNDO) calculations have been carried out for several allotropes, hydrides, and oxides of phosphorus,²¹ including isomers of P_4 , P_6 , and P_8 . MNDO calculations have been performed for a range of molecular fragments derived from P_4S_3 , including P_3 and P_4 ,³⁷ and SINDO1 calculations for P_4 .³⁸ However, we have found no calculations of P_5 and P_7 in the literature and

a systematic search for states other than those with particular symmetries has not been performed for P_n clusters with $n > 3$. We address this problem in the present work.

The difficulties inherent in seeking molecular states with low-lying energies are twofold: (i) determining reliably the total energy E for fixed atomic positions $\{\mathbf{R}_I\}$, (ii) minimizing E with respect to variations in $\{\mathbf{R}_I\}$. The difficulties in calculating E are well known. The determination of the total energy from the exact wave function is very difficult in clusters like P_8 , even for a single geometry, so that a search for global minima using configuration interaction methods is presently unattainable. Even with more efficient energy calculations, however, the location of low-lying minima in the energy surface would remain a problem of enormous complexity. It has been shown³⁹ that the determination of the ground state of a cluster of identical atoms interacting via two-body forces belongs to the class NP ,⁴⁰ i.e., no known algorithm with a polynomial time dependence can solve the problem. For sufficiently small clusters, the global minimum can be determined by locating and enumerating *all* the local minima. However, the search is confined in practice to small parts of configuration space based on expectations, symmetry, or experimental information.

In systems where the ground state is unknown or there are many local minima, it is necessary to develop alternative methods for finding solutions that are near to optimal. One possibility is to adopt a "simulated annealing" technique,⁴¹ where the system of electrons and ions can evolve at finite temperature. The ionic motion means that, as in nature, the system can avoid being trapped in unfavorable local minima in the energy surface. Car and Parrinello⁴² have shown that this strategy can be implemented by combining molecular dynamics (MD) with the density functional (DF) scheme for calculating total energies, leading to a method for calculating electronic properties that makes no assumptions about ground state geometries. MD techniques allow an efficient sampling of the potential energy surface and the DF method⁴³ with the local spin density (LSD) approximation for the exchange-correlation energy, avoids the explicit parametrization of the interatomic forces common in MD schemes.

We have applied this approach to calculate ground state geometries of clusters of selenium ($Se_n, n = 3-8$)⁴⁴ and sulphur ($S_n, n = 2, 13$).⁴⁵ The calculated geometries are in excellent agreement with those cases where x-ray structural analyses have been performed and the predicted structures for the others should be reliable. In the S_7O molecule,⁴⁶ we were able to follow the change of structure from a local minimum with the oxygen atom in the ring (i.e., with a $-S-O-S-$ bridge bond) to the ground state structure of an O atom bonded to an S_7 ring. The method has also been applied with success to study the isomers of Se_xS_y isomers.⁴⁷ The local density approximation used for the exchange-correlation energy results in a systematic overestimate of bonds (by ~ 1 eV per bond in S and Se), so that the bonding trends are given reliably.

The method we use has been described in detail elsewhere⁴⁵ and we give those aspects needed here in Sec. II. In Sec. III, we present our results for P_2 to P_8 and compare the

results with other calculations and with experiment where available. Binding energy and structural trends are presented in Sec. IV and our concluding remarks in Sec. V.

II. METHOD OF CALCULATION

A. The molecular dynamics/density functional (MD/DF) approach

The density functional formalism⁴³ shows that a knowledge of the electron density $n(\mathbf{r})$ is sufficient to determine the ground state properties of a system of electrons in an external field V_{ext} . In particular, the ground state energy E_{gs} can be found by minimizing the relationship between energy and density $E[n]$ and this minimum is found for the ground state density n_{gs} . It is convenient to write⁴⁸

$$E[n] = T_0[n] + \int d\mathbf{r} n(\mathbf{r}) [V_{\text{ext}}(\mathbf{r}) + \frac{1}{2}\Phi(\mathbf{r})] + E_{\text{xc}}[n], \quad (1)$$

where T_0 is the kinetic energy that a system with density n would have in the absence of electron-electron interactions, $\Phi(\mathbf{r})$ is the Coulomb potential, and E_{xc} is the exchange-correlation energy. To evaluate E_{xc} , we adopt the local spin density (LSD) approximation

$$E_{\text{xc}}^{\text{LSD}} = \int d\mathbf{r} n(\mathbf{r}) \epsilon_{\text{xc}}[n_{\uparrow}(\mathbf{r}), n_{\downarrow}(\mathbf{r})], \quad (2)$$

where $\epsilon_{\text{xc}}[n_{\uparrow}, n_{\downarrow}]$ is the exchange and correlation energy per particle of a homogeneous, spin-polarized electron gas with spin-up and spin-down densities n_{\uparrow} and n_{\downarrow} , respectively. While different electron gas calculations result in different forms of ϵ_{xc} , the consequences for calculated geometries and energy differences are relatively small. In the present work, we use the parametrization of Vosko *et al.*⁴⁹ of the quantum Monte Carlo calculations of Ceperley and Alder.⁵⁰

For a given set of atomic coordinates $\{\mathbf{R}_I\}$, the minimization of $E[n]$ in Eq. (1) is usually performed by solving the Kohn-Sham equation

$$\left[\frac{1}{2}\nabla^2 + V_{\text{ext}}(\mathbf{r}) + \Phi(\mathbf{r}) + V_{\text{xc}}(\mathbf{r})\right]\psi_i(\mathbf{r}) = \epsilon_i\psi_i(\mathbf{r}), \quad (3)$$

where $V_{\text{xc}} = \delta E_{\text{xc}}/\delta n(\mathbf{r})$. The density can be constructed from the eigenfunctions of this equation $n(\mathbf{r}) = \sum_i |\psi_i(\mathbf{r})|^2$, with i running over all occupied states. The procedure must be continued until self-consistency is reached. We use a pseudopotential representation of the electron-ion interaction, with the parameters for phosphorus determined by Bachelet *et al.*⁵¹ and the eigenfunctions of Eq. (3) are expanded in a plane wave basis.

In order to optimize the geometry, we view E as a function of two interdependent sets of degrees of freedom $\{\psi_i\}$ and $\{\mathbf{R}_I\}$:

$$E[\{\psi_i\}, \{\mathbf{R}_I\}] = \sum_i \langle \psi_i(\mathbf{r}) | -\frac{\nabla^2}{2} | \psi_i(\mathbf{r}) \rangle + \int d\mathbf{r} n(\mathbf{r}) \left[V_{\text{ext}}(\mathbf{r}) + \frac{1}{2}\Phi(\mathbf{r}) \right] + E_{\text{xc}}[n(\mathbf{r})] + \frac{1}{2} \sum_{I \neq J} \frac{Z_I Z_J}{|\mathbf{R}_I - \mathbf{R}_J|}, \quad (4)$$

where \mathbf{R}_I and \mathbf{Z}_I denote the ionic coordinates and effective charges, respectively. To minimize this function with respect to variations in $\{\mathbf{R}_I\}$, we use a dynamical simulated annealing technique to follow the trajectories of $\{\psi_i\}$ and $\{\mathbf{R}_I\}$ given by the Lagrangian

$$\mathcal{L} = \sum_I \mu_i \int_{\Omega} d\mathbf{r} |\dot{\psi}_i^* \dot{\psi}_i| + \sum_I \frac{1}{2} M_I \dot{\mathbf{R}}_I^2 - E[\{\psi_i\}, \{\mathbf{R}_I\}] + \sum_{ij} \Lambda_{ij} \left(\int_{\Omega} d\mathbf{r} \psi_i \psi_j^* - \delta_{ij} \right) \quad (5)$$

and the corresponding time-dependent equations of motion

$$\mu_i \ddot{\psi}_i(\mathbf{r}, t) = - \frac{\delta E}{\delta \psi_i^*(\mathbf{r}, t)} + \sum_k \Lambda_{ik} \psi_k(\mathbf{r}, t),$$

$$M_I \ddot{\mathbf{R}}_I = - \nabla_{\mathbf{R}_I} E. \quad (6)$$

Here M_I are the ionic masses, μ_i are fictitious “masses” associated with the electronic degrees of freedom, and the Lagrangian multipliers Λ_{ij} are introduced to satisfy the orthonormality constraints on the $\psi_i(\mathbf{r}, t)$. From these orbitals and the resultant density $n(\mathbf{r}, t) = \sum_i |\psi_i(\mathbf{r}, t)|^2$, we use Eq. (4) to evaluate the total energy E , which acts as the classical potential energy in the Lagrangian (5).

B. Computational details

The goal of the present calculations is to locate low-lying minima in the energy surface and the strategy adopted is different from that needed when studying time- and temperature-dependent properties. Calculations were performed for a range of starting geometries in each system and the coordinates were then perturbed by small random amounts to reduce possible bias resulting from the geometry assumed. The velocities $\dot{\psi}_i$ and $\dot{\mathbf{R}}$ are set equal to zero and Eq. (3) solved for this geometry using a small basis set (energy cutoff 27.2 eV). This is the only explicit diagonalization in the calculation. The resulting eigenfunctions serve as input to an iterative steepest descents calculation of ψ_i for this geometry (using the full plane-wave basis). We then alternate steepest descents techniques ($\Delta t = 2.0 \times 10^{-15}$ s, $\mu_i = 50\,000$ a.u.) with MD at $T = 300$ K ($\Delta t = 1.7 \times 10^{-16}$ s, $\mu_i = 300$ a.u. using the Verlet⁵² algorithm) to locate the minimum and probe the local environment of the energy surface. We then perform longer MD runs at several temperatures to ensure that there are no lower-lying minima with similar geometries.

During the MD calculations, the average instantaneous temperature $\langle T \rangle$ —the mean kinetic energy of the ions—is kept constant to within $\sim 5\%$ by rescaling the ionic velocities uniformly with a factor $\sqrt{\langle T \rangle / T}$. The isokinetic ensemble thus simulated will have a different dynamical behavior from the canonical energy distribution probably appropriate for an isolated cluster, but we note again that the focus of the calculations is the energy surface and its minima and not the temperature-dependent properties. The above choice of parameters ensures that the transfer of energy between the ionic and electronic degrees of freedom is small. We found that the electronic system stays within ~ 0.1 eV of the ground state, so that the motion of the system is close to Born–Oppenheimer (BO) trajectories.

We have used a large fcc unit cell [lattice constant 15.9 Å] with constant volume [1000 Å³] and periodic boundary conditions. The separation between individual clusters is large and we have shown in our calculations for S and Se clusters that the results are insensitive to the choice of boundary conditions. The cut-off energy for the plane wave expansion of the electronic eigenfunctions was 5.3 hartree (144.2 eV) during the MD simulated annealing runs, leading to ~ 4000 plane waves for a single point ($\mathbf{k} = 0$) in the Brillouin zone. The convergence of relative energies and cluster geometries has been studied in the case of P₄. With the cut-off energy increased from 144.7 to 285.7 eV, the difference between the total energies of the “roof” and tetrahedral structures increased by 0.06 eV (to 2.25 eV). The bond lengths decreased almost uniformly by 1–1.5%, so that the bond and dihedral angles changed by only 0.1–0.3°. Similar results may be expected in the other clusters. As we noted in the case of sulphur clusters, the total (valence) energy converges more slowly with increasing size of a plane-wave basis.

It is convenient to assume that the angular momentum dependent components of the nonlocal pseudopotential, $V_{ps}^l(\mathbf{r})\hat{P}_l$, satisfy $V_{ps}^l = V_{ps}^{l_{\max}}$ for $l > l_{\max}$, where \hat{P}_l is the projection operator of the l th angular momentum component. In our work on Se_n and S_n, we set $l_{\max} = 1$ and showed that the main effect of increasing l_{\max} was to reduce the bond lengths by a small amount. The very accurate energy differences required in the work on the isomers of Se_xS_y⁴⁷ made it essential to use $l_{\max} = 2$, and we have used this improved approximation in the present calculations. Test calculations have shown, however, that the only significant effect in phosphorus clusters is on the bond length. Energy differences proved to be remarkably insensitive to the choice of l_{\max} .

III. STRUCTURES OF P₂–P₈

In this section, we discuss the structures found for the different molecules. The spectroscopic constants of the ground state of P₂ are given in Table I and the structural

TABLE I. Spectroscopic constants of P₂ (¹Σ_g⁺).

	r_c (a.u.)	ω_e (cm ⁻¹)	D_e (eV)	D_0^0 (eV)
Expt ^a	3.578	780.77	5.08	5.03
HF ^b	3.496	909.1	1.72	...
HF(2 <i>d</i> 1 <i>f</i>) ^c	3.507	...	1.63	...
HF(6-31G*) ^d	3.513	908	1.16	...
CI-SD ^b	3.545	842.8	3.51	...
CI-SDQ(D) ^b	3.575	805.3	4.15	...
CI-SDQ(S) ^b	3.585	792.7	4.29	...
CPF(3 <i>d</i> 2 <i>f</i> 1 <i>g</i>) ^c	3.583	...	4.52	...
MP2 ^d	3.651	...	4.01	...
MP3 ^d	3.587	...	3.62	...
MD/DF ^e	3.56	780	6.17	...

^a Huber and Herzberg (Ref. 53).

^b McLean *et al.* (Ref. 54) S, D, Q denote single, double, and quadruple excitations (D) and (S) include Davidson corrections.

^c Ahlrichs *et al.* (Ref. 24). Coupled pair functional calculations.

^d Raghavachari *et al.* (Ref. 25).

^e This work.

parameters for low-lying states of P_3 – P_8 are given in Tables II–IV. Parameters not given are related by symmetry to values in the tables. Atomization energies are presented in Table V. The results of experimental analyses are given where available and the structures are shown in Figs. 1–7. Where appropriate, we use a cyclic notation for the atoms in each molecule. “Bonds” in the figures correspond to an interatomic separation of < 4.72 a.u. The vibrational density of states can be obtained by Fourier transforming the velocity autocorrelation function and the results are given here for P_2 and P_4 .

TABLE II. Molecular parameters d , α , and γ for low-lying isomers of P_n , $n = 2$ –5. Bond lengths d_{ij} (between atoms i and j) in a.u., bond angles (α_{ijk}) and dihedral angles (γ_{ijkl}) in degrees. Parameters identical by symmetry are excluded.

d	$P_2(D_{\infty h})$	3.56
d	$P_3(D_{\infty h})$	3.68
d	$P_3(D_{3h})$	4.02
α		60°
	$P_3(C_{2v})$	
d_{12}		3.92
d_{23}		4.25
α_2		57.2°
α_1		65.6°
	$P_4(D_{2h})$	
d_{12}		4.27
d_{23}		3.89
α		90.0°
	$P_4(D_{2d})$	
d_{12}		4.04
d_{24}		4.45
α_{124}		56.6°
α_{214}		66.8°
α_{123}		103.8°
γ_{1234}		32.8°
	$P_4(T_d)$	
d		4.17
α		60.0°
γ		70.5°
	$P_5(D_{5h})$	
d		3.95
α		108.0°
	$P_5(C_{2v}, \text{planar})$	
d_{12}		3.93
d_{23}		3.91
d_{34}		4.03
α_2		99.1°
α_3		111.0°
α_1		119.8°
	$P_5(C_{2v})$	
d_{12}		4.16
d_{23}		4.26
d_{34}		4.11
α_{423}		57.7°
α_{234}		61.2°
α_{215}		81.3°
α_{235}		83.8°
α_{124}		90.0°
γ_{2354}		61.8°

TABLE III. Molecular parameters d , α and γ for low-lying isomers of P_6 . Bond lengths d_{ij} (between atoms i and j) in a.u., bond angles (α_{ijk}) and dihedral angles (γ_{ijkl}) in degrees.

	$P_6(D_{6h})$	
d		3.97
α		120.0°
	$P_6(D_2)$	
d_{12}		3.94
d_{23}		3.98
α_2		109.4°
α_1		122.0°
γ_{12}		29.1°
γ_{23}		52.7°
	$P_6(C_{2h})$	
d_{12}		3.99
d_{13}		4.30
d_{14}		4.53
α_{312}		57.4°
α_{123}		65.2°
α_{134}		90.0°
	$P_6(D_{3h})$	
d_{12}		4.23
d_{14}		4.32
α_{213}		60.0°
α_{214}		90.0°
	$P_6(C_{2v})$	
d_{12}		4.21
d_{16}		3.79
d_{23}		4.21
d_{34}		4.17
α_{423}		59.4°
α_{234}		60.3°
α_{235}		92.7°
α_{124}		105.4°
α_1		105.9°
γ_{2354}		53.2°

A. P_2

The low-lying states of the phosphorus dimer have been investigated extensively in the gas phase,⁵³ and the ground state has the same configuration ($^1\Sigma_g^+$) as the ground state of N_2 . The results of selected calculations for this molecule are compared with the experimental spectroscopic parameters in Table I. The deviations from experiment are consistent with past experience. Hartree–Fock (HF) calculations^{24,25,54} underestimate the bond length and overestimate the vibration frequency, and calculations using correlated wave functions^{24,25,54} give improved results as the basis set and the number of configurations are increased. Nevertheless, even the most extensive calculations underestimate the well depth by ~ 0.5 eV. The density functional calculations lead to values of r_e and ω_e in excellent agreement with experiment. Small changes in these values result if we adopt different pseudopotential parameters or extend the size of the plane wave basis. While the almost perfect agreement for the vibration frequency is then somewhat fortuitous, it gives us confidence in our predictions of other structures. The phosphorus atom has a half-filled p shell and the bond in P_2 is the strongest P–P bond known. The overestimate of the well depth by ~ 1 eV is consistent with previous LSD calculations for sp -bonded molecules.^{43,45,55}

TABLE IV. Molecular parameters d , α , and γ for low-lying isomers of P_7 and P_8 . Bond lengths d_{ij} (between atoms i and j) in a.u., bond angles (α_{ijk}) and dihedral angles (γ_{ijkl}) in degrees.

$P_7(C_s)$	
d_{12}	4.11
d_{23}	4.15
d_{34}	4.22
d_{45}	4.21
d_{56}	4.22
d_{67}	4.17
α_{456}	59.2°
α_{123}	59.7°
α_{465}	60.3°
α_1	60.5°
α_{546}	60.5°
α_{327}	94.0°
α_{457}	94.5°
α_{467}	95.9°
α_{234}	104.0°
α_{275}	104.5°
α_{346}	105.2°
γ_{6457}	49.9°
γ_{4567}	50.8°
$P_8(O_h)$	
d	4.32
α	90°
$P_8(D_{2h})$	
d_{12}	4.21
d_{13}	4.18
d_{27}	4.21
α_{123}	59.6°
α_{213}	60.2°
α_{214}	94.0°
α_{127}	117.8°
γ_{1234}	52.1°
$P_8(C_{2v})$	
d_{12}	4.24
d_{17}	4.15
d_{25}	4.16
d_{78}	4.17
α_{617}	58.3°
α_{176}	63.4°
α_{612}	88.6°
α_{123}	104.6°
α_{178}	107.8°

B. P_3

The phosphorus trimer has been identified in the gas phase⁷⁻⁹ with an atomization energy $D_{0,at}^0$ of 7.76 ± 0.2 eV,⁹ so that it is stable by ~ 2.7 eV with respect to dissociation into P_2 and P. It was predicted by Murrell⁵⁶ to have a triangular (possibly D_{3h}) structure and subsequent calculations have confirmed this. The highest occupied molecular orbital in D_{3h} is spatially degenerate (e'') and partially occupied, so that this form of P_3 is subject to a Jahn-Teller distortion. The Hartree-Fock (HF) calculations of Murrell *et al.*³³ show that the distortion is small, with the final C_{2v} structure having a bond length of 4.25 a.u. and a bond angle of 64°. The configuration interaction (CI) energy of the linear form of P_3 ($D_{\infty h}$) is 1.36 eV higher. MNDO calculations³⁷ also produce a C_{2v} ground state, with one short bond of 3.543 a.u. and two long bonds of 3.753 a.u. (a C_{2v} bond angle of 58.3°). The linear structure ($r_{PP} = 3.34$ a.u.) lies 1.62 eV higher.

The structures found in the present calculations are shown in Fig. 1. We find a ground state with C_{2v} symmetry

TABLE V. Calculated atomization energies for $P_n, n = 2-8$, compared with thermodynamically derived values for gas phase P_n (energies in eV).^a

n	E_{at}^{calc}	E_{at}^{therm}	E_{at}^{calc}/n	E_{at}^{therm}/n
2 ($D_{\infty h}$)	6.17	5.03	3.08	2.57
3 ($D_{\infty h}$)	8.28	...	2.76	...
3 (D_{3h})	9.37	...	3.12	...
3 (C_{2v})	9.47	7.76	3.16	2.59
4 (D_{2h})	12.81	...	3.20	...
4 (D_{2d} , roof)	13.40	...	3.35	...
4 (T_d)	15.59	12.44	3.90	3.11
5 (D_{5h})	17.51	...	3.50	...
5 (C_{2v} , planar)	17.73	...	3.55	...
5 (C_{2v})	18.12	...	3.62	...
6 (D_{6h})	21.29	...	3.55	...
6 (D_2)	21.58	...	3.60	...
6 (C_{2h})	22.16	...	3.69	...
6 (D_{3h})	22.58	...	3.76	...
6 (C_{2v})	22.75	...	3.79	...
7 (C_s)	26.76	...	3.82	...
8 (O_h)	29.89	...	3.74	...
8 (D_{2h})	30.91	...	3.86	...
8 (C_{2v} , wedge)	31.66	...	3.96	...

^aReference 9.

($r_{pp} = 3.92$ a.u., $\alpha = 65.6^\circ$). It lies 0.10 eV below the lowest-lying state ($^2E''$) with D_{3h} symmetry, which has a bond length of 4.02 a.u. The lowest-lying state with a linear geometry has a P-P bond length of 3.68 a.u. and lies 1.19 eV above the ground state. The DF calculations give a value for the dissociation energy into $P_2 + P$ of 3.30 eV (exp. 2.7 eV), an overestimate similar to that found in S_3 .⁴⁵

C. P_4

This molecule has been the subject of much study since Bhagavantam performed the first measurements in 1930.¹¹ Early electron diffraction measurements¹³ were consistent with a tetrahedral structure with bond length of 4.18 ± 0.04 a.u. and this value has been refined by vibration-rotation

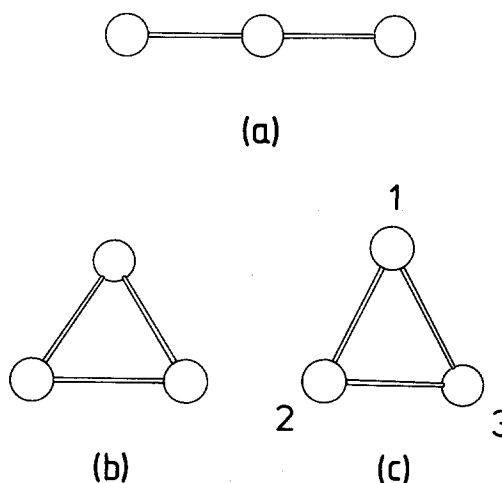


FIG. 1. The structures of P_3 . (a) $D_{\infty h}$; (b) D_{3h} ; (c) C_{2v} .

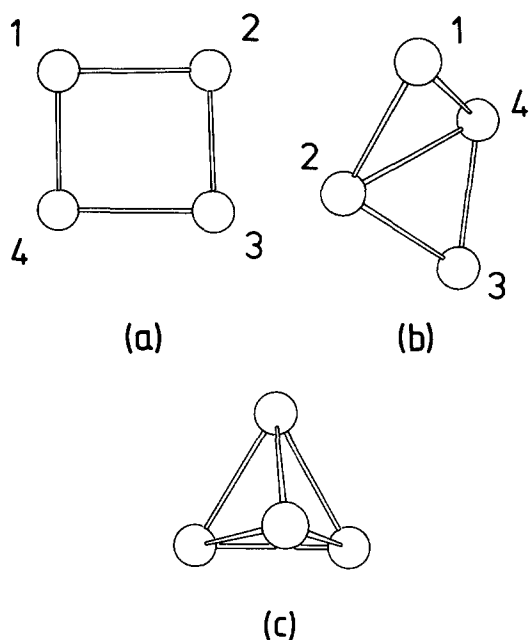


FIG. 2. The structures of P_4 . (a) D_{2h} ; (b) D_{2d} , roof; (c) T_d .

Raman spectroscopy⁵⁷ to 4.2006 ± 0.0009 a.u. The dissociation energies into $P_2 + P_2$ and $P_3 + P$ are 2.37 ± 0.05 and 4.69 ± 0.17 eV, respectively.⁹

Hultgren noted that d -orbitals would favor the T_d structure, but the importance of d functions in describing the bond and the reasons for the apparent relative stability of P_4 have continued to be matters of debate. Brundle *et al.*⁵⁸ performed a HF calculation at the experimental geometry and found excellent agreement with measured ionization potentials using a basis of s - and p -atomic orbitals. They concluded that there is no need for d orbitals in P_4 . A similar conclusion was reached by Seifert and Großmann⁵⁹ on the basis of scattered-wave calculations of P_4 at the experimental geometry. On the other hand, Osman *et al.*¹⁶ found considerable

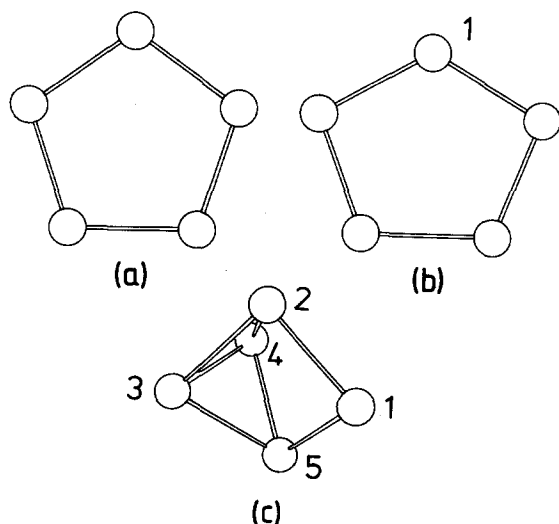


FIG. 3. The structures of P_5 . (a) D_{5h} ; (b) C_{2v} , planar; (c) C_{2v} .

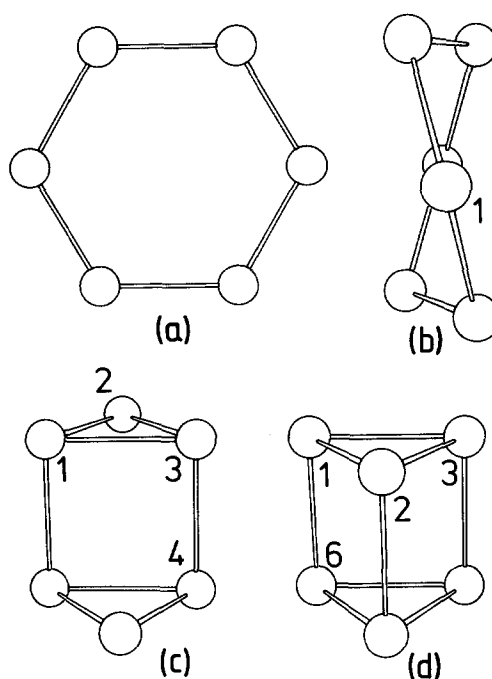


FIG. 4. Four low-lying structures of P_6 . (a) D_{6h} ; (b) D_2 ; (c) C_{2h} ; (d) D_{3h} .

changes in the electron distribution when d functions were included in a HF calculation, and this effect was also observed by Wedig *et al.*¹⁸ Schmidt and Gordon²² and Trinquier *et al.*²³ found that the inclusion of d -basis functions in HF calculations [3-21 G and double zeta (DZ)- d , respec-

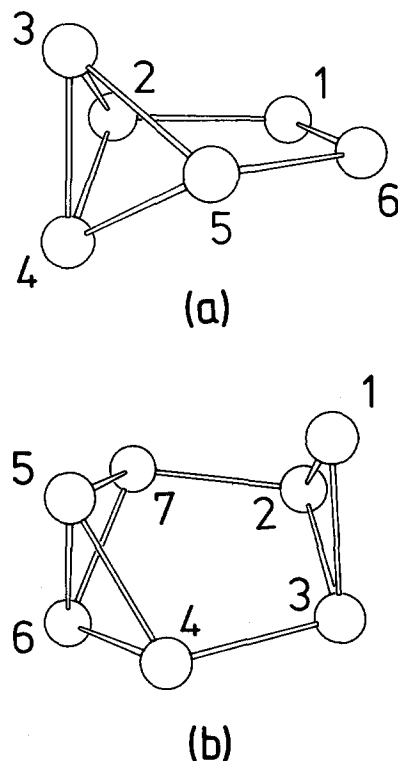
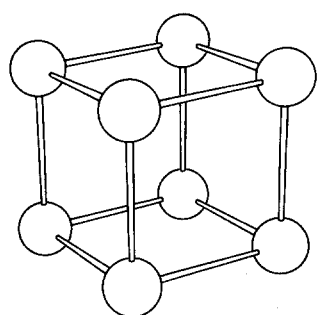
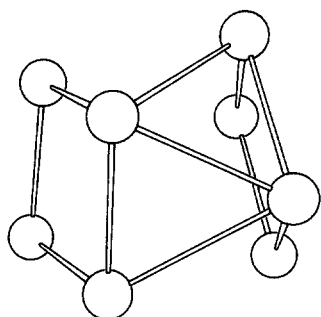


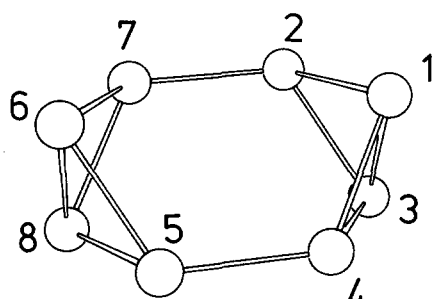
FIG. 5. The structures of the lowest-lying states in (a) $P_6(C_{2v})$; (b) $P_7(C_s)$.



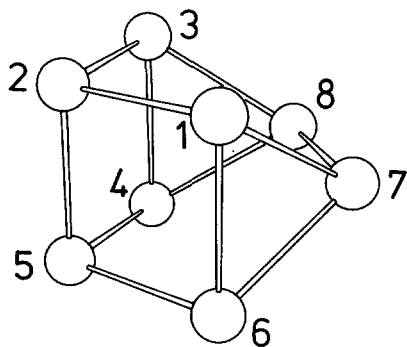
(a)



(b)

FIG. 6. Two P_8 structures. (a) O_h ; (b) C_{2v} .

(a)



(b)

FIG. 7. Two P_8 structures. (a) D_{2h} ; (b) C_{2v} .

tively] led to much improved bond lengths, and Lazzeretti and Tossell⁶⁰ showed that d functions are needed to obtain a reliable estimate of ^{31}P nuclear magnetic resonance shielding constants in P_4 . We conclude that d functions are essential for a quantitative description of the bonding in P_4 .⁶¹

A second problem that has been addressed by several authors is the energy and path of dissociation of $\text{P}_4 \rightarrow \text{P}_2 + \text{P}_2$. The most recent *ab initio* calculations with extended basis sets reproduce both the experimental geometry (T_d) and dissociation energy of P_4 very well. Ahlrichs *et al.*²⁴ find that CPF ($2d\ 1f$) calculations lead to a bond length of 4.17 a.u. and a dissociation energy of 2.08 eV, while third-order Hartree–Fock–Møller–Plesset (HF–MP3) (6-31G*) calculations²⁵ lead to 4.16 a.u. and 1.36 eV, respectively. Similar results were found by Schmidt and Gordon.²² Raghavachari *et al.*²⁵ showed that increasing the basis set to 6-31G($2df$) and using fourth-order Møller–Plesset perturbation theory gave a dissociation energy (2.46 eV) in excellent agreement with experiment. These results show that quantitative computation of the reaction energy $\text{P}_4 \rightarrow 2\text{P}_2$ requires a basis set with f orbitals and at least third-order perturbation theory.

The actual path in configuration space taken during dissociation is difficult to study. Osman *et al.*¹⁶ calculated the energy change on separating two P_2 units along the direction normal to both bonds, and found an activation energy for the process of 1.78 eV. This process and several others were considered in MNDO calculations of Bock and Müller.¹⁰ The smallest increase in MNDO total energy was found for a path involving the breaking of four bonds and the simultaneous shortening of two, i.e., the transition state has D_{2d} symmetry. The height of the barrier between P_4 and 2P_2 was 1.83 eV.

The three structures corresponding to local minima in the energy surface are shown in Fig. 2. As expected, the most stable is the tetrahedral (T_d) structure and the calculated bond length (4.17 a.u.) is in excellent agreement with experiment. The calculated dissociation energy (3.26 eV) reflects the tendency of the LSD approximation to overestimate the stability of structures that are sp bonded. The coordinates of the converged T_d geometry were displaced by random amounts of magnitude less than 0.1 a.u. and the subsequent constant energy MD evolution followed for 6000 time steps. The calculated vibration frequencies ($e = 366\text{ cm}^{-1}$, $t_2 = 448\text{ cm}^{-1}$, $a_1 = 597\text{ cm}^{-1}$ compare very well with the experimental values⁶² (367.2, 462.2, and 606.5 cm^{-1} , respectively).⁶³ The deviations are well within the limits to be expected from either DF/LSD or more traditional quantum chemical calculations.

The least stable P_4 structure evolved from a linear chain and comprises two P_2 molecules weakly bound in a planar zig-zag configuration. A planar rectangular (D_{2h}) structure with bond length of 3.89 and 4.27 a.u. has a stable local minimum, although a shallow one. On “heating” the cluster to an average internal temperature of 500 K, it can overcome a small potential energy barrier and reach the basin of attraction of a “roof” (D_{2d}) structure. The latter can be cooled to 0 K with the annealing strategy described above and is 2.19 eV above the T_d structure and 0.60 eV more stable than the

rectangular geometry. We find that the planar D_{3h} structure (as in SO_3) deforms continuously into the D_{2d} structure and is not a stable local minimum.

We have performed a high-temperature ($T = 15\,000$ K) simulation on the T_d structure of P_4 , the high temperature being chosen to compensate for the short physical times presently attainable. The path taken by the system in configuration space (not the path of least action) corresponds to an opening of two bonds on opposite sides of the tetrahedron, with a continuous decrease in the dihedral angle around one of these bonds. In this simulation, the maximum energy of the system was ~ 4 eV above the ground state energy, so that the height of the barrier in the potential energy surface will be lower. The system then passes over into the basin of attraction of the roof structure, i.e., cooling the molecule and using the annealing plus steepest descents strategy leads to the same energy and geometry as stated above for the D_{2d} structure.

Our calculations show that although the tetrahedral structure of P_4 is by far the most stable, there is a large basin of attraction for the roof structure. This is an interesting result, since we shall see that the P_4 group with D_{2d} symmetry is a constituent of energetically favorable structures in larger clusters.

D. P_5

The P_5 molecule has not been identified in the gas phase at high temperatures and we are unaware of any calculations for the neutral molecule. The polyphosphide ion P_5^- has, however, been identified by Baudler *et al.*²⁷ as a ring of unsubstituted twofold coordinated P atoms. MNDO calculations have been performed for this ion by Baird,²¹ who found a planar pentagonal (D_{5h}) structure with bond length 3.58 a.u.

As in the case of P_3 , the highest occupied molecular orbital in the planar symmetric (D_{5h}) form of P_5 is spatially degenerate and our calculations confirm a Jahn–Teller distortion to a structure of lower symmetry (C_{2v}) and energy. The structure with full D_{5h} symmetry has a bond length of 3.95 a.u. and the parameters of the undistorted and Jahn–Teller distorted structures are given in Table II. The distortion is not large, the largest changes in bond length and bond angle being 0.08 a.u. and 11.8° , respectively, and the energy lies 0.22 eV below the energy of the D_{5h} structure.

The most stable P_5 structure we have found is the C_{2v} structure shown in Fig. 3(c). It lies 0.39 eV in energy below the distorted pentagon and comprises the roof structure of P_4 with a twofold coordinated fifth atom. The bonds to this atom are at 90° to each of the four bonds outlining the roof. We also found two structures corresponding to shallow local minima in the energy surface. A D_{3h} propellerlike structure, with three atoms symmetrically placed with respect to a central bond of length 4.52 a.u., lies 1.57 eV above the ground state. A C_{4v} structure, with a P atom placed centrally above a P_4 square, has an energy 0.45 eV above that of the ground state. However, these structures convert to the C_{2v} state on annealing at 500 K by crossing small energy barriers to the basin of attraction of the ground state minimum.

E. P_6

The P_6^+ ion was found by Martin¹⁴ using mass spectroscopy of quenched phosphorus vapor. Furthermore, Scherer *et al.*²⁸ have prepared a sandwich complex $\{(\eta^5 - \text{Me}_5\text{C}_5\text{Mo})_2(\mu, \eta^6 - \text{P}_6)\}$ with the planar hexagonal form (D_{6h}) occupying the central bridge position. This form of P_6 is isoelectronic with benzene and it is interesting to speculate on its possible existence.²⁸ There have been several attempts to calculate the relative energies of different isomers of P_6 , motivated in part by this question and by the possibility of synthesizing the molecule from P_2 units. Baird²¹ performed MNDO calculations on three forms of P_6 . The most stable is the prismane (D_{3h}) analog. The benzene analog lies 0.22 eV higher and a C_{2v} structure lies a similar amount above that. Baird found that the predicted heats of formation per atom were comparable to those observed for P_4 .

The same three isomers were treated in the HF approximation by Nagase and Ito.³⁵ The most extensive calculations with a 6-31G* basis indicated that the three isomers had very similar energies, with the C_{2v} structure being the most stable. Nguyen and Hegarty³⁶ have performed HF calculations with Møller–Plesset corrections to compare the energies of P_6 (D_{6h}) and 3P_2 . They predicted that the former lies 6 kcal mol^{-1} (0.25 eV) above 3P_2 and would decompose $\text{P}_6 \rightarrow 3\text{P}_2$ with an energy barrier of 13 kcal mol^{-1} (0.56 eV).

We have found several structures corresponding to local minima in the energy surface [Figs. 4 and 5(a)]. The minimum for the planar hexagon (D_{6h}) is shallow and converts on annealing to the D_2 structure shown in Fig. 4(b). The latter structure has a projection that is very similar to Fig. 4(a). It is, in fact, a modest perturbation of the D_{6h} structure, lying 0.29 eV below it and 0.58 eV above the C_{2h} structure shown in Fig. 4(c). Of the structures considered by other authors, we found the structure analogous to prismane (D_{3h}) to be the most stable. The most stable isomer, however, was found to be a C_{2v} structure derived from the P_5 ground state by replacing the single atom outside the D_{2d} roof by a dimer [Fig. 5(a)]. It is analogous to the benzvalene isomer of $(\text{CH})_6$ ^{64,65} and lies 0.17 eV below the prismane structure in our calculations. This small energy difference means that both structures are candidates for the ground state. Preliminary calculations in As_6 (Ref. 66) indicate, e.g., that the D_{3h} structure is the most stable in this molecule. The octahedral structure was found to be unstable, reverting on annealing at 300 K to the C_{2h} structure [Fig. 4(c)].

F. P_7

It was only recently that P_7^+ was detected in the gas phase¹⁴ and we are not aware of any attempts to predict its geometry using either *ab initio* or semiempirical methods. We noted above that the P_7^- ion has been synthesized and provides an interesting example of valence bond tautomerism, where the molecule fluctuates continuously between structures with different bonding configurations above a certain temperature.

In our search for the ground state structure of the neutral P_7 cluster, we found a shallow local minimum in the energy surface for a capped prism (C_{2v}), derived from the P_6

(D_{3h}) structure, with a seventh atom bonded to the four atoms in one face. This structure is unstable towards thermal treatment at 300 K and converts to the only stable minimum we have found in this molecule (C_s) under these conditions [Fig. 5(b)]. The corresponding minimum at $T = 0$ shows again the P_4 -roof structure, bonded to a P_3 unit that is close to equilateral. In order to study further the stability of this structure, we have performed extended simulated annealing runs (a total of 40 000 time steps at temperatures between 300 and 3000 K). There were substantial changes in geometry, including distortions of the P_4 roof such that one atom moved closer to the apex angle of the triangle. This structure approximates that of P_7^{3-} or the isoelectronic tetraphosphorus trisulphide P_4S_3 .⁶⁷ It is, however, energetically unfavorable and reverts to the most stable structure described above.

G. P_8

This molecule has been detected in the vapor phase at low temperatures¹⁴ and between 100 and 300 °C,^{6,8} but is not present at higher temperatures.^{7,10} As noted above, calculations of the molecule have been restricted to the cubic (O_h) form, on the assumption that the most favorable, strain-free bonding configuration of phosphorus is p^3 , with three mutually orthogonal bonds. Geometry optimizations have been performed for this structure only at the HF level and lead to a consistent picture. The bond lengths found are 4.286 a.u. (6-31G*),²⁵ 4.330 a.u. (1d),²⁴ 4.280 a.u. (3-21G*),²² and 4.297 a.u. (DZ-d).²³ The energy of the reaction $2P_4 \rightarrow P_8$ is 1.52, 1.63, 1.50, and 1.14 eV, respectively. In the most detailed calculations incorporating correlation effects (the MP3 calculations of Raghavachari *et al.*²⁵), this energy is increased to 2.41 eV, so all calculations predict that the cubic form of P_8 lies well above the energy of two P_4 molecules. The calculated vibration frequencies are all real,^{22,23,25} so that the O_h structure is a local minimum on the P_8 potential energy surface. While Schmidt and Gordon²² viewed this as proof of the cubic structure of P_8 , Raghavachari *et al.*²⁵ noted that the low vibrational frequency might indicate the existence of a "soft" reactive channel. The latter is consistent with our findings.

The present calculations show that the O_h structure is a local minimum in P_8 , with a bond length of 4.32 a.u. [Fig. 6(a)]. If we perturb the coordinates of each atom by a random number of magnitude less than 0.02 a.u. and perform a steepest descents calculation of the potential energy surface, the structure returns to the cubic form. The cube is therefore a locally stable minimum in our study and the energy of the reaction $2P_4 \rightarrow P_8$ (1.29 eV) is in satisfactory agreement with the estimates of the *ab initio* calculations. If we anneal the cubic structure at $T = 200$ K, however, it undergoes a shear deformation, leading to a local minimum with an energy 0.25 eV below that of the cube. The structure is shown in Fig. 6(b).

An extended thermal treatment of a cubic starting structure with bond length 4.05 a.u. (10 000 time steps at $T = 300$ K) has also been carried out. After an initial distortion simi-

lar to that shown in Fig. 6(b), the total energy dropped much farther and the combination of annealing and steepest descents calculations resulted in a structure with an energy 1.77 eV below that of the cubic structure. The final structure [Fig. 7(b)] can be understood most simply as a cube with one P–P bond rotated through 90° and is the most stable P_8 structure we have found. In order to study its stability, we have performed another extended series of molecular dynamics runs (10 000 time steps at temperatures between 1000 and 9000 K). Using the technique of alternating annealing with steepest descents calculations, we obtained an identical structure, with an energy less than 0.0001 a.u. different. This demonstrates the stability of the minimum and provides us with an estimate of the reliability of the calculated energy differences. The energy of the calculated ground state is 0.47 eV below that of two isolated P_4 tetrahedra. A further isomer, with a second bond rotated through 90°, lies 0.75 eV above the ground state [see Fig. 7(a)], still well below the cube. This structure (D_{2h}) comprises two P_4 roof tetramers and it is interesting to note that the bonds between the tetramers are the same length as the adjoining bonds in the four-atom units.

The structures and energetics of the new isomers of P_8 were unexpected. However, the C–H group is isoelectronic with P and similar structures are well known and of particular interest in hydrocarbon chemistry.^{64,65} The cubic form of $(CH)_8$, known as "cubane," was synthesized by Eaton and Cole,⁶⁸ and could be catalyzed to a second isomer with a shape as in Fig. 7(b) using silver or palladium.⁶⁹ In view of the wedgelike structure, Cassar *et al.*⁶⁹ used the term "cuneane" to describe it. They estimated that it should be ~30–40 kcal mol⁻¹ less strained than cubane and that the strain energy of the third possible isomer [2,2':4,4'-bis-(bicyclobutyl)] should be intermediate between these values.⁶⁹ The ordering of strain energies in the $(CH)_8$ isomers would then be the same as we find for the total energies in P_8 isomers. Furthermore, the structure of violet (monoclinic) phosphorus comprises long tubes of pentagonal cross section containing P_8 and P_9 "cages," connected by pairs of phosphorus atoms.^{1,30} Although the presence of the dimers presents a constraint on the structure, the P_8 units have the same basic form as our ground state for the isolated P_8 molecule. A similar eight-membered structure is found in realgar (As_4S_4) in both the gaseous⁷⁰ and crystalline⁷¹ forms, and has been referred to as a "cradle" configuration.

Further simulations have been performed on this molecule, with interesting results. An initial structure similar to the D_{4h} "crown" in S_8 deforms readily into one P_2 and two P_3 units, with short (and therefore strong) bonds between them. This is a further demonstration of the preference of phosphorus to form structures with threefold coordination. During the formation of the triangles, however, the "bonds" to the remaining two atoms became very long. We have noted this effect in the course of simulations on several of the molecules, i.e., the formation of a structure with more favorable coordination was often associated with a weakening of bonds in the structure. This process could result in dissociation of the molecule at elevated temperatures.

IV. BINDING ENERGY AND STRUCTURAL TRENDS

The calculated atomization energies are given in Table V, together with experimental values where available. The tendency of DF/LSD calculations to overestimate bond strengths in *sp*-bonded materials is well known^{43,55} and this is evident in our results for P_2 , P_3 , and P_4 . Experience with numerous families of molecules has shown, however, that the bonding *trends* are generally reliable, and we study these here.

We have found a number of local energy minima in each cluster, as well as minima in the potential energy surface that are too shallow to constrain the molecule at $T = 300$ K. The predictions for the ground state geometries in P_5 – P_8 show that structures with a P_4 roof unit are energetically favored in all cases. In P_5 , we have an additional P atom bonded to two atoms in the roof, and in P_6 , P_7 , and P_8 the extra atom is replaced by a dimer, trimer, and a second P_4 roof, respectively. The changes in the dihedral angle formed by the four atoms in the tetramer are consistent with this picture. The $P_4(T_d)$ structure has a value of $\gamma = 70.5^\circ$ and opening this structure to accommodate an atom and a dimer leads to dihedral angles of 61.8° and 53.2° in P_5 and P_6 , respectively. Smaller changes in γ are required for the corresponding structures in P_7 and P_8 . While the double-roof structure in P_8 is more stable than the well-studied cubic form, we find that the “wedge” or “cradle” form is the most stable isomer in this molecule.

The total (valence) energies per atom are shown for all structures in Fig. 8. We note that there is an overall trend for increasing stability as n increases, so that P_n clusters should be stable (at $T = 0$) for all $n < 8$. This is consistent with the detection by Martin¹⁴ of P_n^+ clusters for all n in this range. The smallest energy difference is the value noted above for

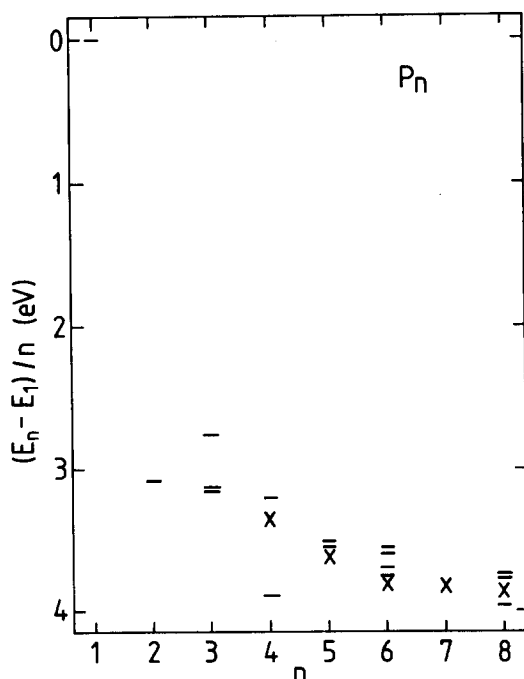


FIG. 8. Total (valence) energies per atom of P_n structures shown in Table V. The structures with roof components are shown by crosses.

the energy of the most stable P_8 isomer relative to two P_4 tetrahedra. Martin also observed an oscillation in the relative abundances of P_n^+ clusters with increasing n and noted that highly stable clusters have an even number of electrons. Our results (Fig. 8) are consistent with this. The particularly strong bond in P_2 reflects the occupancy of all bonding orbitals, while the $P_4(T_d)$ structure has threefold coordination of *all* atoms and a larger ratio of bonds per atom (6:4) than its neighbors. The crosses in Fig. 8 show that the relative stabilities of the roof structures increase smoothly with increasing n .

The roof or open tetrahedron structure played a role in the discussion of Pauling and Simonetta¹⁵ concerning the formation of red phosphorus from the white form, which comprises weakly bound P_4 tetrahedra. These authors noted that the breaking of one bond in a tetrahedron could result in a figure formed by two equilateral triangles with a common base. The two apical P atoms would then form bonds to similar atoms in adjacent P_4 complexes, forming chains of the form $(P_4)_n$. Half of the atoms would form bonds with two 60° bond angles and one 101° bond angle, and the other half with one 60° and two 101° bond angles. Pauling and Simonetta estimated that this structure would be more stable than white phosphorus and noted that the relative ease of forming red phosphorus compared with the most stable (black) form could be understood from the fact that only one P–P bond needs to be broken. A similar polymerization process was mentioned by Elliott *et al.*³² as a way of generating the P_8 cages they identified in amorphous red phosphorus. Our calculations indicate that the $P_8(D_{2h})$ structure is ~ 0.3 eV less stable than two P_4 tetrahedra. Since we are comparing energy differences involving the same number of bonds¹² of approximately equal length, we expect that the LSD estimate should be reliable.

Trends in bond lengths and angles in phosphorus have been noted by several authors. The orthorhombic allotrope is composed of puckered layers, within each of which the P atoms are threefold coordinated. The bond lengths are 4.20 (twice) and 4.24 a.u. (once), with bond angles 96.3° (once) and 102.1° (twice).¹ The layers in the rhombohedral structure have bonds with $r_{PP} = 4.03$ a.u. and $\alpha = 105^\circ$, and the cubic form of black phosphorus has $r_{PP} = 4.49$ a.u., $\alpha = 90^\circ$. For structures with bond angles near 90° , the shortest bonds then correlate with the largest departures from a right angle. The cage structures present in violet (monoclinic) phosphorus result in a distribution of bond lengths into three groups. As pointed out by Thurn and Krebs,^{1,30} there is a correlation between bond distances and the dihedral angles about the bond. The average of the bond lengths in “eclipsed” configurations (one dihedral angle $\gamma \sim 0^\circ$) is significantly longer (4.30 a.u.) than in “staggered” ($\gamma \sim 90^\circ$ – 120°) or “trans” (one value of $\gamma \sim 180^\circ$) configurations (4.23 and 4.16 a.u., respectively). Although the data on clusters are not extensive, similar trends are apparent. The weakness of the bond in cubic P_8 , e.g., has been attributed in part to the presence of parallel bonds.^{19,24}

The structures found in the present work show some interesting trends, with an obvious preference for threefold coordination. Fourfold structures such as pyramids and oc-

tahedra proved to be unstable under annealing at low temperatures and twofold structures such as planar forms [$P_4(D_{2h})$, $P_5(D_{5h})$, $P_6(D_{6h})$] were generally energetically unfavorable. The bond angles in Table V show an interesting distribution. The occurrence of roof and triangular structures leads naturally to a peak in the bond angle distribution near 60° and structures related to the cubic ordering lead to values near and above 90° . The most stable isomer in P_8 has fewer parallel bonds than the cubic structure studied previously and the bond angles α_{123} and α_{178} show significant changes from 90° . It is striking that the structures found in the present work show almost no bond angles between 60° and 90° . The bond angle distribution calculated by Hafner⁷² for isoelectronic liquid As shows a similar trend, with peaks at 60° and 94° and a long tail to larger values of α . This last feature was not observed in the present cluster study and may be an artifact of the pairwise additive interatomic potentials applied to the liquid, and the corresponding lack of higher order interactions.

V. CONCLUDING REMARKS

We have described calculations of the energy surfaces of phosphorus molecules using the MD-DF method, which requires no assumptions about the equilibrium structure. While thermodynamic data are available for P_2 , P_3 , and P_4 , structures and vibration frequencies are presently known only for P_2 and P_4 . The calculated structures and frequencies are in excellent agreement with the measured ones and the atomization energies show the overestimates familiar from previous DF work using the LSD approximation (2) for the exchange-correlation energy. Previous theoretical work on these systems has been restricted to P_2 , P_3 , and to particular symmetries of P_4 , P_6 , and P_8 . Special interest has been paid to the energy of the reaction $P_8(O_h) \rightarrow 2P_4(T_d)$.

The structures and relative energies found in the present work were unexpected, and may surprise many. A significant number of the structures we have found for P_n clusters are known in the analogous structures for $(CH)_n$,^{64,65} but the differences between phosphorus and the methine group mean that the ordering of the most stable isomers may differ. An example is $(CH)_6$, where benzene is more stable than benzvalene.⁶⁵ The reverse is true in the P_6 calculations. We find minima in the energy surfaces for all P_n clusters with $n < 8$, with a trend to increasing stability for increasing n . The tetrahedral structure of P_4 is particularly stable and we confirm previous findings that two P_4 tetrahedra are less stable than the cubic form of P_8 . The wedge-shaped isomer of P_8 is more stable than two tetrahedra, but the energy difference is less than 0.5 eV. Our calculations indicate that all P_n clusters ($n < 8$) should exist at low temperatures and this finding is consistent with the recent identification of singly ionized clusters up to $n = 24$ in quenched phosphorus vapor.¹⁴ All previously published work had been performed at elevated temperatures, indicating that the larger clusters are thermally unstable. This shows again the value of techniques such as laser vaporization and cooling by supersonic expansion, which have resulted in cluster beams with low internal temperatures.

It would be of great interest to see whether more tradi-

tional methods for molecular electronic structure calculations confirm our findings on the geometries and relative stabilities of the clusters studied here.⁷³ Our calculations provide further evidence for the complexity of the energy surfaces of molecules and we have found stable minima corresponding to geometries that were surprising and previously unexplored. Even with gradient expansions of the energy, it is not clear that zero-temperature methods will be able to find a path between relevant energy minima in clusters of this size. The introduction of a kinetic energy ("temperature") term in Eq. (5) enables the system to locate some of the most favorable geometries in a large region of configuration space. The short time scale currently accessible using the simulated annealing technique means that there are regions that are not probed by this method. Although the present series of calculations has been very extensive, there can be no guarantee that other important minima do not exist. Application of the method to clusters of arsenic is in progress.

ACKNOWLEDGMENTS

We thank R. Car and M. Parrinello for valuable discussions and P. S. Bechthold for bringing Ref. 14 to our attention after the original manuscript had been submitted. We also thank the German Supercomputer Center (Hochleistungsrechenzentrum, HLRZ) for a grant of computer time on the Cray Y-MP 832 in the Forschungszentrum Jülich.

¹J. Donohue, *The Structures of the Elements* (Wiley, New York, 1974), Chap. 9.

²D. E. C. Corbridge, *The Structural Chemistry of Phosphorus* (Elsevier, Amsterdam, 1974).

³D. E. C. Corbridge, *Phosphorus. An Outline of its Chemistry, Biochemistry and Technology*, 3rd ed. (Elsevier, Amsterdam, 1985).

⁴T. P. Martin, *J. Chem. Phys.* **81**, 4427 (1984).

⁵R. Steudel, in *Studies in Inorganic Chemistry*, edited by A. Müller and B. Krebs, Eds. (Elsevier, Amsterdam, 1984), Vol. 5, p. 3.

⁶L. Kerwin, *Can. J. Phys.* **32**, 757 (1954).

⁷J. S. Kane and J. H. Reynolds, *J. Chem. Phys.* **25**, 342 (1956).

⁸J.-D. Carette and L. Kerwin, *Can. J. Phys.* **39**, 1300 (1961).

⁹J. Smets, P. Coppens, and J. Drowart, *Chem. Phys.* **20**, 243 (1977).

¹⁰H. Bock and H. Müller, *Inorg. Chem.* **23**, 4365 (1984).

¹¹S. Bhagavantam, *Indian J. Phys.* **5**, 35 (1930).

¹²R. Hultgren, *Phys. Rev.* **40**, 891 (1932).

¹³L. R. Maxwell, S. B. Hendricks, and V. M. Mosley, *J. Chem. Phys.* **3**, 699 (1935).

¹⁴T. P. Martin, *Z. Phys. D* **3**, 211 (1986).

¹⁵L. Pauling and M. Simonetta, *J. Chem. Phys.* **20**, 29 (1952).

¹⁶R. Osman, P. Coffey, and J. R. van Wazer, *Inorg. Chem.* **15**, 287 (1976).

¹⁷E. Fluck, C. M. E. Pavlidou, and R. Janoschek, *Phosphorus and Sulphur* **6**, 469 (1979).

¹⁸U. Wedig, H. Stoll, and H. Preuss, *Chem. Phys.* **61**, 117 (1981).

¹⁹G. Trinquier, J.-P. Malrieu, and J.-P. Daudey, *Chem. Phys. Lett.* **80**, 552 (1981).

²⁰E. A. Halevi, H. Bock, and B. Roth, *Inorg. Chem.* **23**, 4376 (1984).

²¹N. C. Baird, *Can. J. Chem.* **62**, 341 (1984).

²²M. W. Schmidt and M. S. Gordon, *Inorg. Chem.* **24**, 4503 (1985).

²³G. Trinquier, J.-P. Daudey, N. Komihira, *J. Am. Chem. Soc.* **107**, 7210 (1985).

²⁴R. Ahlrichs, S. Brode, and C. Ehrhardt, *J. Am. Chem. Soc.* **107**, 7260 (1985).

²⁵K. Raghavachari, R. C. Haddon, and J. S. Binkley, *Chem. Phys. Lett.* **122**, 219 (1985).

- ²⁶M. Baudler, *Angew. Chem.* **94**, 520 (1982).
- ²⁷M. Baudler, D. Düster, and D. Ouzounis, *Z. Anorg. Allg. Chem.* **544**, 87 (1987).
- ²⁸O. J. Scherer, H. Sitzmann, and G. Wolmershäuser, *Angew. Chem. Int. Ed. Engl.* **24**, 351 (1985).
- ²⁹W. Höhle and H. G. von Schnering, *Z. Allg. Anorg. Chem.* **440**, 171 (1978).
- ³⁰H. Thurn and H. Krebs, *Acta Crystallogr. Sect. B* **25**, 125 (1969).
- ³¹G. Fasol, M. Cardona, W. Höhle, and H. G. von Schnering, *Solid State Commun.* **52**, 307 (1984).
- ³²S. R. Elliott, J. C. Dore, and E. Marseglia, *J. Phys. Colloq. C* **8** **46**, 349 (1985).
- ³³J. N. Murrell, O. Novaro, S. Castillo, and V. Saunders, *Chem. Phys. Lett.* **90**, 421 (1982).
- ³⁴O. Novaro and S. Castillo, *Int. J. Quantum Chem.* **26**, 411 (1984).
- ³⁵S. Nagase and K. Ito, *Chem. Phys. Lett.* **126**, 43 (1986).
- ³⁶M. T. Nguyen and A. F. Hegarty, *J. Chem. Soc., Chem. Commun.* **1986**, 383.
- ³⁷J. R. Bews and C. Glidewell, *J. Mol. Struct. (Theochem)* **86**, 217 (1982).
- ³⁸K. Jug, R. Iffert, and J. Schulz, *Int. J. Quantum Chem.* **32**, 265 (1987).
- ³⁹L. T. Wille and J. Vennik, *J. Phys. A* **18**, L419 (1985); **18**, L1113 (1985).
- ⁴⁰M. R. Garey and D. S. Johnson, *Computers and Intractability: A Guide to the Theory of NP Completeness* (Freeman, San Francisco, 1979).
- ⁴¹S. Kirkpatrick, C. D. Gelatt, and M. P. Vecchi, *Science* **220**, 671 (1983).
- ⁴²R. Car and M. Parrinello, *Phys. Rev. Lett.* **55**, 2471 (1985); **60**, 204 (1988); P. Ballone, W. Andreoni, R. Car, and M. Parrinello, *ibid.* **60**, 271 (1988).
- ⁴³For a review, see R. O. Jones and O. Gunnarsson, *Rev. Mod. Phys.* **61**, 689 (1989).
- ⁴⁴D. Hohl, R. O. Jones, R. Car, and M. Parrinello, *Chem. Phys. Lett.* **139**, 540 (1987).
- ⁴⁵D. Hohl, R. O. Jones, R. Car, and M. Parrinello, *J. Chem. Phys.* **89**, 6823 (1988).
- ⁴⁶D. Hohl, R. O. Jones, R. Car, and M. Parrinello, *J. Am. Chem. Soc.* **111**, 825 (1989).
- ⁴⁷R. O. Jones and D. Hohl, *J. Am. Chem. Soc.* (in press).
- ⁴⁸W. Kohn and L. J. Sham, *Phys. Rev.* **140**, A1133 (1965).
- ⁴⁹S. Vosko, L. Wilk, and M. Nusair, *Can. J. Phys.* **58**, 1200 (1980).
- ⁵⁰D. M. Ceperley and B. J. Alder, *Phys. Rev. Lett.* **45**, 566 (1980).
- ⁵¹G. B. Bachelet, D. R. Hamann, and M. Schlüter, *Phys. Rev. B* **26**, 4199 (1982).
- ⁵²L. Verlet, *Phys. Rev.* **159**, 2471 (1967).
- ⁵³K. P. Huber and G. Herzberg, *Molecular Spectra and Molecular Structure. IV. Constants of Diatomic Molecules* (Van Nostrand-Reinhold, New York, 1974).
- ⁵⁴A. D. McLean, B. Liu, and G. S. Chandler, *J. Chem. Phys.* **80**, 5130 (1980).
- ⁵⁵O. Gunnarsson and R. O. Jones, *Phys. Rev. B* **31**, 7588 (1985).
- ⁵⁶J. N. Murrell, *Chem. Phys. Lett.* **55**, 1 (1978).
- ⁵⁷N. J. Brassington, H. G. M. Edwards, and D. A. Long, *J. Raman Spectrosc.* **11**, 346 (1981).
- ⁵⁸C. R. Brundle, N. A. Kuebler, M. B. Robin, and H. Basch, *Inorg. Chem.* **11**, 20 (1972).
- ⁵⁹G. Seifert and G. Großmann, *Z. Chem. (Leipzig)* **6**, 233 (1978).
- ⁶⁰P. Lazzeretti and J. A. Tossell, *J. Phys. Chem.* **91**, 800 (1987).
- ⁶¹See also W. Kutzelnigg, *Angew. Chem.* **96**, 262 (1984).
- ⁶²Y. M. Bosworth, R. J. H. Clark, and D. M. Rippon, *J. Mol. Spectrosc.* **46**, 240 (1973).
- ⁶³These frequencies are not vacuum corrected. A more precise value of ν_e ($360.813 \pm 0.004 \text{ cm}^{-1}$) has been derived from the vibration-rotation Raman spectrum by N. J. Brassington, H. G. M. Edwards, and D. A. Long, *J. Raman Spectrosc.* **11**, 346 (1981).
- ⁶⁴A. T. Balaban, *Rev. Roum. Chim.* **11**, 1097 (1966).
- ⁶⁵L. T. Scott and M. Jones, Jr., *Chem. Rev.* **72**, 181 (1972).
- ⁶⁶R. O. Jones and D. Hohl (unpublished).
- ⁶⁷J. D. Head, K. A. R. Mitchell, L. Noodleman, and N. L. Paddock, *Can. J. Chem.* **55**, 669 (1977).
- ⁶⁸P. E. Eaton and T. W. Cole, Jr., *J. Am. Chem. Soc.* **86**, 962 (1964); **86**, 3157 (1964).
- ⁶⁹L. Cassar, P. E. Eaton, and J. Halpern, *J. Am. Chem. Soc.* **92**, 6366 (1970).
- ⁷⁰C.-S. Lu and J. Donohue, *J. Am. Chem. Soc.* **66**, 818 (1944).
- ⁷¹T. Ito, N. Morimoto, and R. Sadanaga, *Acta Crystallogr.* **5**, 775 (1952).
- ⁷²J. Hafner, *Phys. Rev. Lett.* **62**, 784 (1989).
- ⁷³Coordinates of the structures obtained in the present work are available on request.